New Phytologist

Research

Flower production decreases with warmer and more humid atmospheric conditions in a western Amazonian forest

Jason Vleminckx[1,2,3], J. Aaron Hogan[4], Margaret R. Metz[5], Liza S. Comita[3], Simon A. Queenborough[3], S. Joseph Wright[6], Renato Valencia[7], Milton Zambrano[7] and Nancy C. Garwood[8]

[1]Department of Biology of Organisms, Université Libre de Bruxelles, Brussels, 1050, Belgium; [2]Yale Institute for Biospheric Studies, Yale University, New Haven, CT 06511, USA; [3]School of the Environment, Yale University, New Haven, CT 06511, USA; [4]Department of Biology, University of Florida, Gainesville, FL 32611, USA; [5]Department of Biology, Lewis & Clark College, Portland, OR 97219, USA; [6]Smithsonian Tropical Research Institute, Apartado, Balboa, 0843-03092, Panama; [7]Escuela de Ciencias Biológicas, Pontificia Universidad Católica del Ecuador, Quito, 170143, Ecuador; [8]School of Biological Sciences, Southern Illinois University, Carbondale, IL 62901, USA

Author for correspondence:
Jason Vleminckx
Email: *jasvlx86@gmail.com*

Received: *1 June 2023*
Accepted: *18 October 2023*

New Phytologist (2023)
doi: 10.1111/nph.19388

Key words: climate change, flower production, lowland Amazonian everwet tropical forests, plant reproduction, relative humidity, solar irradiance, temperature, western Amazonia.

Summary

- Climate models predict that everwet western Amazonian forests will face warmer and wetter atmospheric conditions, and increased cloud cover. It remains unclear how these changes will impact plant reproductive performance, such as flowering, which plays a central role in sustaining food webs and forest regeneration. Warmer and wetter nights may cause reduced flower production, via increased dark respiration rates or alteration in the reliability of flowering cue-based processes. Additionally, more persistent cloud cover should reduce the amounts of solar irradiance, which could limit flower production.
- We tested whether interannual variation in flower production has changed in response to fluctuations in irradiance, rainfall, temperature, and relative humidity over 18 yrs in an everwet forest in Ecuador.
- Analyses of 184 plant species showed that flower production declined as nighttime temperature and relative humidity increased, suggesting that warmer nights and greater atmospheric water saturation negatively impacted reproduction. Species varied in their flowering responses to climatic variables but this variation was not explained by life form or phylogeny.
- Our results shed light on how plant communities will respond to climatic changes in this everwet region, in which the impacts of these changes have been poorly studied compared with more seasonal Neotropical areas.

Introduction

There is growing evidence that climate change is altering the ecology of tropical forest plant communities around the world (Sullivan *et al.*, 2020). Although climate changes are global, they are of particular importance in the forests of Amazonia because of the area's outstanding biodiversity and crucial role in the global carbon cycle (Pan *et al.*, 2011). Tipping points beyond which these forests will experience a dramatic loss of resilience and stop acting as carbon sinks may be reached under a scenario of 1.5°C warming (Sterck *et al.*, 2016; IPCC, 2022; Parry *et al.*, 2022). Such a level of warming may be associated with an increasing frequency of dramatic droughts, especially in the most eastern and southern parts of the Amazon Basin (Fu *et al.*, 2013; Duffy *et al.*, 2015; Marengo *et al.*, 2018; Parsons, 2020; IPCC, 2022). However, the robustness of these predictions is limited by the lack of *in situ* meteorological measurements and by the complexity of the spatiotemporal climatic variability and the interplay among climate variables across the Amazon region (Parsons, 2020; Fassoni-Andrade *et al.*, 2021). For instance, since the 1980s, studies have reported increasing precipitation trends in the western Amazonian Basin, and decreasing trends in the eastern basin (Duffy *et al.*, 2015; Haghtalab *et al.*, 2020; Fassoni-Andrade *et al.*, 2021; Fleischmann *et al.*, 2023). In fact, the last IPCC report (IPCC, 2022) predicts no clear trend in total annual rainfall in western Amazonia, though it suggests an increase in heavy rainfall events (e.g. maximum 5-d precipitation) in the region, especially beyond 1.5°C warming.

In addition to these reports on rainfall, studies have documented increasing cloud cover during the period 1980–2016 in the western Amazon Basin (Jimenez *et al.*, 2018). If this trend continues, forests located in the most everwet and clouded areas of the region may experience a decrease in both the amount of, and seasonal variation in, solar irradiance, with potential negative consequences on primary productivity (Loescher *et al.*, 2003), as well as on the reliability of solar irradiance as a cue for phenological events like flowering (Wright & Calderon, 2018).

Warming might be particularly threatening for tropical forest plants, which currently experience temperatures close to their thermal optimum of photosynthesis (Doughty & Goulden, 2008;

Crous *et al.*, 2022; Vinod *et al.*, 2022). Daytime temperatures exceeding this optimum may affect species' performance through increased metabolic costs and potential thermal damage in the leaves (Perez & Feeley, 2018). At night, rising temperatures induce greater dark respiration rates (Slot *et al.*, 2014), which result in greater carbon loss and reduced biomass productivity at the whole-plant level (Cavaleri *et al.*, 2008). Additionally, warmer nighttime conditions may disrupt plant phenological responses if a threshold minimum temperature or a duration below a certain temperature is a proximate cue to synchronise flowering or fruiting, a phenomenon that has been reported among dipterocarp species in Asia (Satake *et al.*, 2019; Numata *et al.*, 2022) and other tree species in Africa (Tutin & Fernandez, 1993).

Temperature may also interact with changes in air humidity to influence forest phenology and productivity. High relative humidity decreases the vapor pressure gradient along the soil–plant–atmosphere continuum, thereby reducing water demand and plant transpiration rate (Damour *et al.*, 2010; Grossiord *et al.*, 2020). Warmer and more water-saturated atmospheric conditions reduce transpiration and evaporative cooling and thus increase dark respiration rate and potential leaf photosynthetic damage, with detrimental consequences for growth and reproduction (Tibbitts, 1979; Krause *et al.*, 2010). Lin *et al.* (2017) have even suggested that everwet tropical forests might be more at risk for moisture-induced reduced transpiration than dry tropical forests.

The impacts of changing climate conditions on tree growth and mortality have been well studied (Williamson *et al.*, 2000; Needham *et al.*, 2018; Aleixo *et al.*, 2019). However, their effects on tree reproduction (i.e. flower and seed production) remain uncertain (Cook *et al.*, 2012; Pau *et al.*, 2018). Yet, species regeneration and whole forest productivity and dynamics, as well as the nature and quantity of food sources for higher trophic levels, depend on the successful production of flowers and fruits (Van Schaik *et al.*, 1993). A previous study showed that rising atmospheric CO_2 concentration increased flower production from 1987 to 2013 in a seasonal moist tropical forest of Panama (Pau *et al.*, 2018). In the same location, higher daytime temperature has been shown to coincide with higher flower production, potentially through faster photosynthetic activity or more rapid litter decomposition (Pau *et al.*, 2013). Recent evidence suggested that tropical plant species may have a greater margin of resilience than previously expected before reaching temperatures beyond their thermal photosynthetic optima (Smith *et al.*, 2020), which would support a positive effect of high daytime temperature on tree productivity and reproduction.

Because flower production is energy-demanding, it might be limited by the amount of photosynthetically active radiation. In particular, the everwet forests of western Amazonia, close to the equator, are covered by thick convective clouds of the Intertropical Convergence Zone (Min *et al.*, 2004; Pau *et al.*, 2013). These thick clouds reduce irradiance reaching the forest canopy, limiting daily temperature. However, they could also limit nocturnal temperature drop through an enhanced cloud-mediated glasshouse effect (Allan, 2011), which may potentially maintain high temperature-dependent respiration rates that could reduce primary productivity and thus, indirectly, also reduce flower production (Perez & Feeley, 2018). An important question, then, is how flower production changes in response to variation in solar irradiance, atmospheric temperatures, relative humidity, and rainfall.

Here, we examine variation in five climate factors (irradiance, rainfall, minimum and maximum air temperature, and average relative air humidity) over an 18-yr period (2000–2018) in a 50-ha everwet tropical forest dynamics plot in western Amazonia. We analyse how these factors have influenced flower production of 184 woody plant species. We formulate the following hypotheses, in light of the literature described above: (1) an increase in relative air humidity and nighttime (minimum) temperature would negatively impact flower production, and the negative effect of minimum temperature would increase with relative humidity (and vice versa) because transpiration and evaporative cooling decrease with increasing atmospheric moisture. (2) Regarding the effect of daytime (maximum) temperature, we aligned our predictions with Pau *et al.* (2013) who emphasised a positive effect on flower production (we thus assumed that photosynthesis operates sufficiently lower than its thermal optimum among species to detect a positive temperature effect). (3) A decrease in irradiance would negatively impact flower production if the latter is light-limited or if high-light levels are a proximate cue for flowering. (4) Rainfall being *a priori* nonlimiting in the study region (mean monthly rainfall always exceeds 100 mm), we expected that interannual variation in rainfall would have no direct influence on flower production. Finally, we also explored how flowering responses differed among species and tested whether such differences were explained by life form guild and phylogeny.

Materials and Methods

Study site

The Estación Científica Yasuní (ECY, 0°41′S, 76°24′W) is a biological field station affiliated with the Pontificia Universidad Católica del Ecuador. The station is located within Yasuní National Park (YNP; Fig. 1). The YNP represents, with the adjacent Huaorani Ethnic Reserve, the largest protected area (1.6 M ha) of mature tropical forest in the Ecuadorian Amazon (Valencia *et al.*, 2004a). The region is dominated by evergreen, terra firme moist forest situated at about 200 m above sea level, standing on eroded landscapes characterised by undulating and modestly steep relief (Berdugo *et al.*, 2022). The canopy stretches from 15 to 30 m high, with emergent trees reaching up to 50 m (Valencia *et al.*, 2004a). Soils from the Yasuní area are mainly composed of sediments originating from the erosion of the Andes (Malo & Arguello, 1984) and lake formation and marine incursions that occurred during the Miocene (Hoorn *et al.*, 2010). These events may have largely contributed to the habitat heterogeneity of the region, which may have promoted speciation

Fig. 1 Geographical location of the Yasuní Forest Dynamic Plot (FDP) in the Yasuní National Park (YNP; darker grey area).

events and thereby partly explain the outstanding species richness of the Andean Amazon region (Baraloto *et al.*, 2021).

The phenological and climate data were collected in the 50-ha Yasuní Forest Dynamics Plot (YFDP). This plot was established in 1995 to map, identify, measure, and tag all trees ≥ 1 cm in diameter at 1.3 m aboveground (DBH), approximately every 5 yr (Valencia *et al.*, 2004a,b). The plot contains a hyperdiverse flora, comprising 1104 tree and shrub species inventoried in a 25-ha portion during the initial census (Valencia *et al.*, 2004b), including 40 species of *Miconia* (Melastomataceae), 40 species of *Inga* (Fabaceae), and 16 species of Myristicaceae (Valencia *et al.*, 2004b; Queenborough *et al.*, 2007). More details on the YFDP and the paleohistory of the region are available in Netherly (1997) and Valencia *et al.* (2004b).

The YNP is in one of the most humid regions of the Amazon basin (Funatsu *et al.*, 2021). Mean annual rainfall in the park averaged 3165 mm between 2000 and 2018, with a mean monthly rainfall range of 190–375 mm, peak rainfall in April–May, and a secondary peak in October–November (Pitman, 2000; Valencia *et al.*, 2004a). The climate can thus be classified as aseasonal following Walter *et al.* (1975) or everwet following McGregor & Niewold (1998), as monthly rainfall always exceeds 100 mm. Over the same period, mean monthly temperature minima, average, and maxima ranged between 20.9 and 22.0, 24.1 and 25.6, and 29.5 and 32.1°C, respectively.

Climate measurements and climate variation across years

Solar irradiance (measured in Wm^{-2}), rainfall (mm), and temperature (°C) were recorded hourly at ECY from May 2000 to February 2012 using two LI-COR LI-200S pyranometers (calibrated for the daylight spectrum, 400 to 1100 nm), a LI-1400-102 air temperature sensor, a LI-1400-106 tipping bucket, and a Li-1400 data logger (LI-COR Inc., Lincoln, NE, USA; Garwood *et al.*, 2023). Relative humidity was recorded from January 2008 by a LI-COR 1400-04 sensor. In 2012, the equipment was completely replaced by a CR1000 data logger (Campbell Scientific, Logan, UT, USA), two Vaisala HMP45C, one Rotronic HC2-S3 temperature/relative humidity sensors, a Hydrological Services TB4 precipitation gauge, and two LI-COR LI-200X pyranometers (calibrated for the daylight spectrum, 400–1100 nm). This second set of equipment recorded irradiance and temperature measurements every 5 minutes, from January 2012 to February 2018. Rainfall was measured daily using a manual gauge during the same period.

Due to technical issues related to the difficulty of maintaining the equipment in a remote location like YNP, there were gaps in the meteorological data. Missing data at the daily level ranged from 26 to 29% for temperature, rainfall, and irradiance, to 61% for relative humidity (Supporting Information Fig. S1). There were 2189 out of 6633 d (33%) with measurements made for all

climate variables, and 1193 out of 6633 d (18%) with data missing for all variables. Lacking data were scattered across the study period for irradiance, rainfall, and temperature, whereas relative humidity measurements were lacking for the first 8 yr of the study period (Fig. S2).

We imputed missing data using Bayesian hierarchical probabilistic matrix factorisation (BHPMF), after standardising (*z*-score transformation) then normalising (Box-Cox transformation) observed values for each climate variable. BHPMF is a machine-learning algorithm that exploits hierarchical information from structured data and uses their correlation to impute missing entries (Schrodt *et al.*, 2015). We used the month of the year and the day of the month as proxies to structure the data imputation. *Post hoc* analyses showed high robustness in the estimation of imputed data (mean of the distribution of 10 000 imputed values): The SD of the standardised imputed values' distribution never exceeded 1.3 among days with missing climate data, and there was high consistency in the correlation among variables before and after imputation (Fig. S3). These analyses showed that imputations performed well and allowed us to use continuous climate time series for irradiance, rainfall, temperature, and relative humidity (Fig. S2). Since we formulated different hypotheses regarding the potential effects of nighttime and daytime temperatures on flower production, we used minimum daily temperature (hereafter, T_{MIN}) and maximum daily temperature (T_{MAX}) data, separately, in our analyses. For the relative humidity, we only considered the average daily values (hereafter RH_{AVE}), because we lack specific hypotheses regarding the effects of nighttime vs daytime relative humidity on tree reproduction, and because imputations may produce unrealistic values when using variables with values close to a mathematical limit (Rodwell *et al.*, 2014), like maximum relative humidity (max. 100%).

Phenological data

Flowering activity was monitored at the YFDP using the stationary trap methodology of Wright & Calderon (1995). Two hundred horizontal traps of 0.75 × 0.75 m (0.57 m^2) made of 1-mm fibreglass wire mesh were placed throughout the YFPD at 0.75 m aboveground (Garwood *et al.*, 2023). Traps were inventoried approximately every 2 wk from February 2000 to February 2018 (435 censuses). During each census, all flowers were identified and recorded to the nearest order of magnitude (1, 10, 100, or 1000) for each trap. We combined hermaphroditic, female, or male flower fragments into a single 'flower presence' for each species. Morphospecies were assigned a unique code before further taxonomic identification, based on local reproductive adults and our permanent voucher collection (Valencia *et al.*, 2004a; Garwood *et al.*, 2023).

Following Wright & Calderon (2006), we limited our analyses to the community of flowering species present in at least 10 of the 200 traps and in at least 10 out of the 18-yr study period. This resulted in a dataset comprising a total of 184 species, of which 167 (90%) were present in at least 14 yr with no gaps of two or more consecutive years (Fig. S4). These species included 127 genera and 50 families. The families represented by the largest numbers of species were Fabaceae (32 species, including 14 *Inga* species), Meliaceae (12), Euphorbiaceae (11), and Sapindaceae (10). In terms of life form guilds, 87 species were classified as emergent or canopy trees, 44 as climbers, and 53 as understory trees or shrubs. The list of species with their family, life form guild, and additional sampling information is provided in Dataset S1.

Data analysis

Flower production and climate variable values We quantified the total annual flower production of: each species (hereafter, F_{SPE}); and of the whole community (F_{COM}), separately. For each species, F_{SPE} corresponded to the sum (natural log-transformed) of the number of traps in which its flowers were recorded. Since there are 200 traps and 24 censuses in a year, there is a maximum of 4800 trap–census combinations per species per year. F_{SPE} thus quantifies the number of trap–census combinations in a year, with years aligned with species-specific flowering phenologies. It is important to define species-specific phenological years because flowering occurs year-round at Yasuni. Calendar years arbitrarily divide flower production associated with a single flowering event between two calendar years for species that flower from December into January. Species-specific phenological years avoid this problem and are calculated as follows. Day of the year (DOY) is a linear variable, which takes all integer values between 0 and 364. We determined the value of DOY for every trap–census combination and calculated the variance of DOY for each species using the entire 18-yr record. We will refer to DOY_0 if DOY equals 0 on 1 January and 364 on 31 December. The variance of DOY_0 is large for species that flower from December into January. We then obtained DOY_1 by shifting the values of DOY_0 by one calendar day, assigning 363 to 31 December, 364 to 1 January, 0 to 2 January, etc. We repeated this process to find the minimum of the variances of DOY_0, DOY_1, …, DOY_{364}. Finally, species-specific phenological years begin on the calendar date assigned the value 0 for the minimum variance. If several consecutive calendar dates have the same minimum variance, the species-specific phenological year begins at the midpoint. The mean values of each climate variable were calculated for each phenological year and were used in regression models to explain F_{SPE} (see Methods section).

To calculate annual flower production at the community level (F_{COM}), we first standardised the number of trap–census combinations to proportions, for each species separately, by dividing the number of trap–census combinations for each census by the total number of trap–census combinations summed over all censuses. Standardisation was done separately for each species so that all species were on the same scale. For each of the 432 censuses, we then summed the standardised values across species and calculated the starting day of the phenological year, following the method described in the previous paragraph for F_{SPE}. The mean values of each climate variable were calculated for the single community-level phenological year and used in regression models to explain F_{COM} (see Methods section). The mean monthly

flower production and the starting phenological month of each species is shown in Fig. S5.

Flower production response to each climate variable We quantified the year-level effect of each of the eight climate variables (solar irradiance, rainfall, minimum, average and maximum temperature, and minimum, average, and maximum relative humidity) on F_{COM} and F_{SPE}. To do so, we calculated the slope coefficient of the climate variable in an ordinary least square (OLS) linear model. Ordinary least square models were chosen because the residuals were normally or quasi-normally distributed. We also verified the relative performance of generalised linear models using a Poisson or a negative binomial link function and found that the latter models showed a lower or comparable correlation between model-predicted (fitted) values and observed values compared with OLS models.

In the first set of analyses, eight OLS models were performed for F_{SPE} for each species and for F_{COM}. Each model included a single climate variable as the predictor. The regression slope coefficient quantifying the effect of a climate variable was tested by comparing its observed value with 4999 null values obtained using a procedure based on Moran spectral randomisations (MSR, Wagner & Dray, 2015). Here, the MSR used information on temporal connectivity among censuses to account for multiscale temporal (intra- and interannual) autocorrelation structures in the climate variable. This information was obtained from an optimised selection of Moran's eigenvector maps (MEMs, Dray *et al.*, 2006), following Bauman *et al.* (2018a,b). Moran's eigenvector maps are vectors that allow the modelling of multiscale structures (e.g. spatial, temporal, and phylogenetic) in any quantitative variable. In the MSR method, the connectivity information (here, temporal connectivity) is then used in a constrained randomisation algorithm to reproduce a null climate variable with a temporal structure that accurately mimics the observed temporal structure of the randomised climate variable. As an illustration, a visual comparison between the temporal variation of the observed irradiance and the variation of an MSR-randomised irradiance is shown in Fig. S6.

Depending on our *a priori* hypothesis for the sign of the expected correlation between flower production and a climate variable, the slope of each model was considered significantly positive (for irradiance, rainfall, and maximum temperature), or significantly negative (for minimum temperature and relative humidity), when its value was positive and higher than the 95th percentile, or negative and less than the 5th percentile of null values generated using the MSR procedure, respectively (unilateral tests with α-significance threshold of 0.05). We did not correct for multiple tests considering their number (eight tests for the F_{COM}, and 184 species × eight variables = 1472 tests for the F_{SPE}). Instead, when analysing the F_{SPE}, we calculated and compared the proportion of significant negative and positive slope coefficients among species for each climate variable. We considered that 10% was an acceptable type I error rate threshold, meaning that proportions of significant coefficient values higher than 10% indicated that there were reasonably more species responding to the climate variable than expected by chance.

The flower production response to each climate variable was compared among three life form guilds (emergent/canopy trees, climbers, and shrubs/understory trees). We tested the phylogenetic signal of these responses using a testing procedure of Pagel's lambda statistic (see details in Notes S1).

Testing the interaction term in OLS models comprising two climate predictors In a second set of OLS models, we further examined how the effect of one climate variable on F_{COM} depended on the value of another climate variable. More specifically, based on our *a priori* hypothesis about the interactive effects of temperature and relative humidity, we evaluated the possibility that F_{COM} responded more (or less) positively or negatively to increasing values of one variable when the values of the other variable were relatively low or high. To do so, we tested the slope of the interaction term of multiple regression (OLS) models constructed as follows:

$$F_{COM} = \alpha^{*}C1 + \beta^{*}C2 + \gamma^{*}C1^{*}C2 + I + \varepsilon \qquad \text{Eqn 1}$$

where α and β are the slope coefficients of the partial effects of climate variables C1 and C2, respectively, γ is the slope of the interaction term, and I and ε corresponded to the intercept and the residuals of the model, respectively. C1 and C2 corresponded to the following pairs of climate predictors: T_{MIN} and RH_{AVE} (Model 1), and T_{MAX} and RH_{AVE} (Model 2); each slope coefficient was tested by comparing its observed value with 4999 null values obtained using the MSR procedure described above. In Model 1, we expect the slope coefficient of each term to be negative according to our hypotheses (unilateral tests). We chose an α-significance threshold of 0.05; slope values were considered significantly negative if they were negative and lower than 95% of null coefficient values. In Model 2, the slope coefficient of RH_{AVE} and the interaction term were tested with the same predictions (negative slope), while we tested whether the coefficient for T_{MAX} was significantly positive (i.e. if it was positive and higher than 95% of null coefficient values).

All analyses were performed in R v.3.6.3 (www.r-project.org). We provide the climate, the phenological data, and the R code (containing the references for the function packages used), to reproduce our analyses in Datasets S2–S5; Methods S1.

Results

Community-level analyses

Over the 18-yr study period, community-level flower production (F_{COM}) increased slightly from 2000 to 2007, followed by a decline in 2018, with an overall negative trend (Fig. 2a). Over the same period, we observed a marked increase in minimum temperature (T_{MIN}; Fig. 2d), as well as in average relative humidity (RH_{AVE}; Fig. 2f), along with a decrease in solar irradiance (Fig. 2b). Maximum temperature (T_{MAX}) also increased (Fig. 2e), although weakly, while no clear interannual trend was observed for rainfall (Fig. 2c).

Among the simple OLS regression models (i.e. the models using a single climate predictor), F_{COM} was significantly

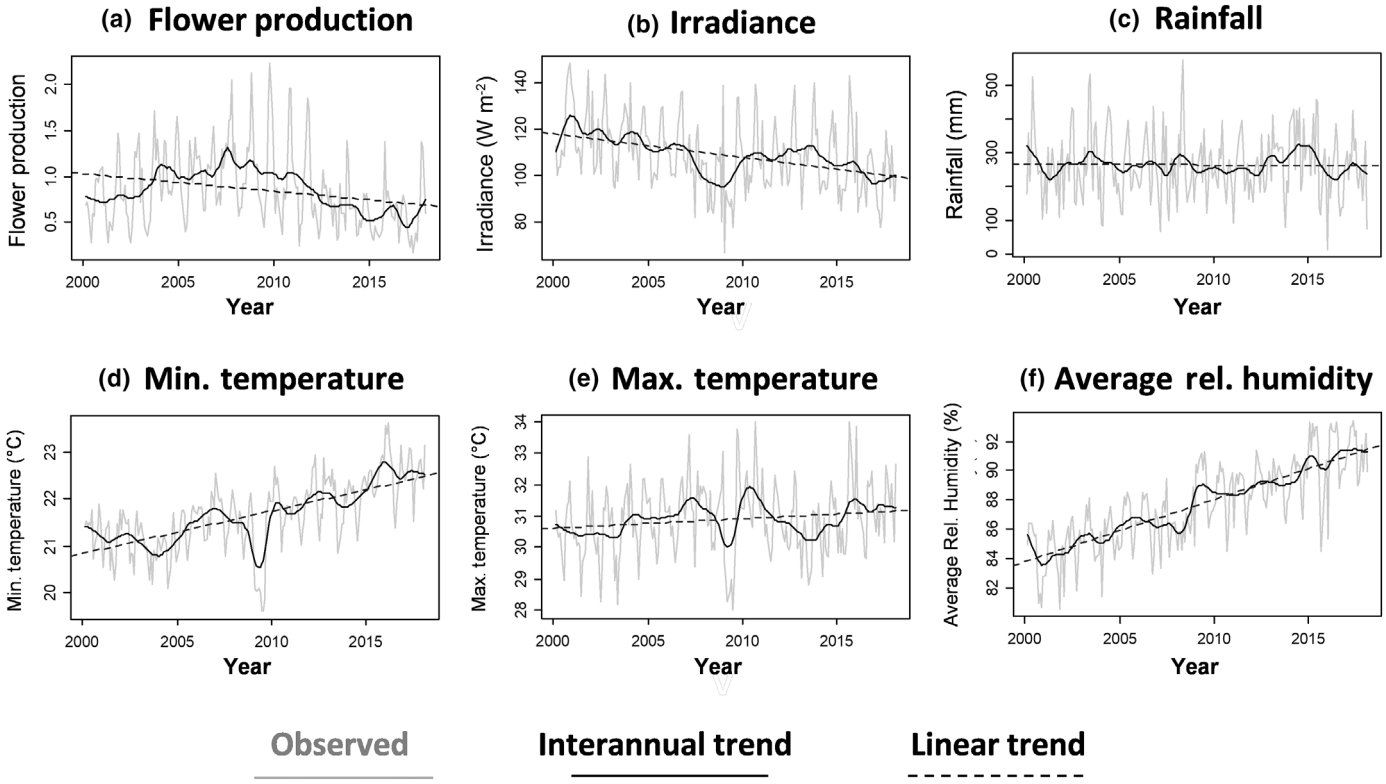

Fig. 2 Monthly variation (grey line) and interannual trend (black line) obtained from Seasonal-Trend Decomposition using Loess (Cleveland *et al*., 1990) for the community-level flower production (a) and each climate variable (b–f) between January 2000 and February 2018. The black dotted line in each graph represents the linear regression trend.

negatively related to T_{MIN} and RH_{AVE} (slope coefficient = −0.64 and −0.49, respectively, with $P = 0.003$ and 0.022; MSR test; Fig. 3c,e); no significant slope coefficient was detected for the three remaining climate variables (Fig. 3a,b,d). We further verified whether a lagged effect of 1 yr for each climate variable on flower production was lower or higher than without any lag. One-year-lagged predictors explained less variation in flower production than nonlagged predictors for T_{MIN} and RH_{AVE} (Fig. S7).

The multiple OLS regression models included the following climate predictors: T_{MIN} and RH_{AVE} (Model 1), and T_{MAX} and RH_{AVE} (Model 2; Fig. 4). Only the first model showed a significantly negative slope coefficient for the interaction term (−0.57; $P = 0.034$; Fig. 4c), such that RH_{AVE} and T_{MIN} effects were both clearly negative at relatively high T_{MIN} and RH_{AVE} values and weakly positive at lower T_{MIN} and RH_{AVE} values (Fig. 4d,e). Model 2 showed significant partial effects ($P \leq 0.016$), being positive for T_{MAX} (0.58; Fig. 4f) and negative for RH_{AVE} (−0.82; Fig. 4g). The interaction effect was not significant (−0.47; $P = 0.068$; Fig. 4h), though we noticed a marked negative effect of RH_{AVE} at warmer T_{MAX} (Fig. 4i), and a pronounced positive effect of T_{MAX} at lower RH_{AVE} (Fig. 4j).

Species-level analyses

Climate variables showing at least 10% of significant negative or positive effects on flower production across species (F_{SPE}) were (in decreasing order of percentage): T_{MIN}, RH_{AVE}, T_{MAX}, and irradiance (Fig. 5a,c–e). There were nearly six times more species responding significantly negatively than positively to T_{MIN} (18.3% vs 3.2%; Fig. 5c) and four times more species for RH_{AVE} (17.7% vs 4.3%; Fig. 5e). For T_{MAX}, the proportion of species responding significantly positively was nearly 24 times higher than the proportion of species responding significantly negatively (12.9% vs 0.54%; Fig. 5d), while it was about two times higher for irradiance (12.9% vs 5.4%; Fig. 5a). We found no significant differences among life form guilds in species response to any climate variable, and no phylogenetic signal was observed for any of these responses (Notes S1; Figs S8 and S9).

Discussion

Over an 18-yr period in an everwet equatorial lowland forest in western Amazonia, we observed a linearly declining trend in community-level flower production, particularly from 2008 to 2018. This trend in flowering paralleled a similar decrease in solar irradiance at the site. By contrast, temperature and relative humidity tended to increase over the same period. The combination of warmer and wetter atmospheric conditions over the years, especially at night, may have negatively impacted flower production. If these trends continue, the decline in reproductive output may alter tree regeneration dynamics as well as reduce fruit resources for animals and humans that depend on these forests for food.

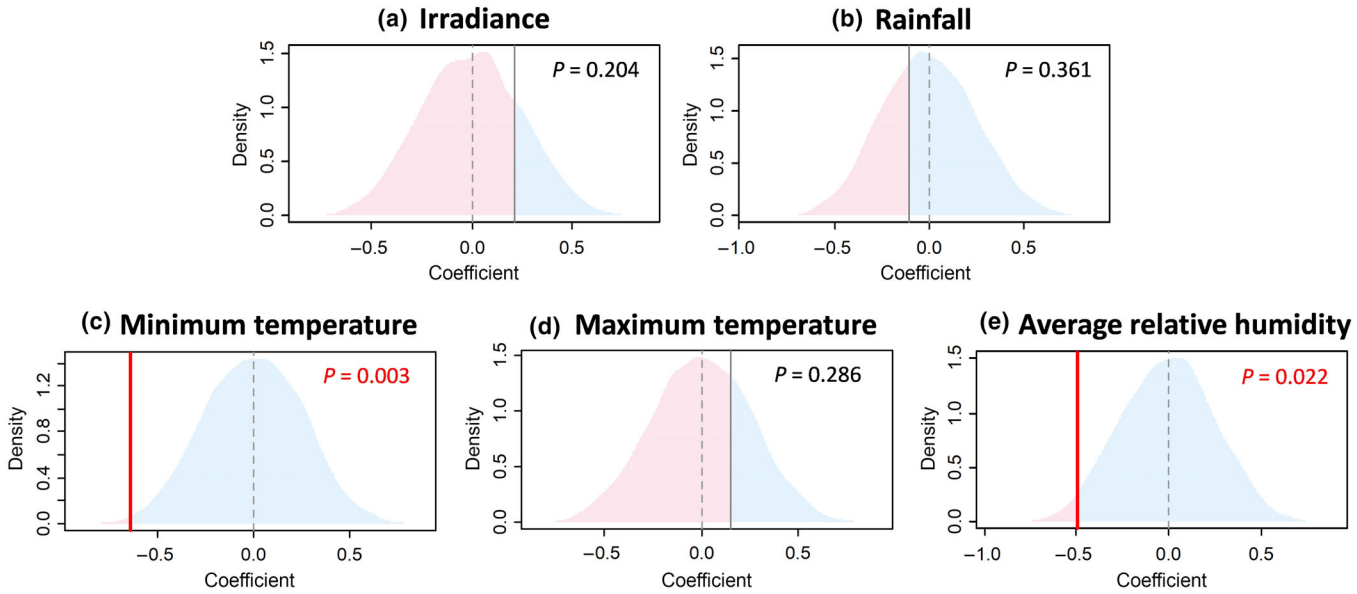

Fig. 3 Density distributions of null slope coefficient values quantifying the effect of each climate variable (a–e) on the annual community flower production (F_{COM}), in each of the eight simple OLS models (i.e. the models that include a single climate predictor). Null values were obtained using the MSR procedure (4999 randomisations). Density distributions are centred on 0 (dashed line). The solid vertical line represents the observed coefficient value. *P* quantifies the proportion of null slope values higher or lower than the observed slope when the latter is positive or negative, respectively. This proportion was < 0.05 for T_{MIN} and RH_{AVE}, only (the vertical bar corresponding to the observed slope coefficient is marked in red for these two variables).

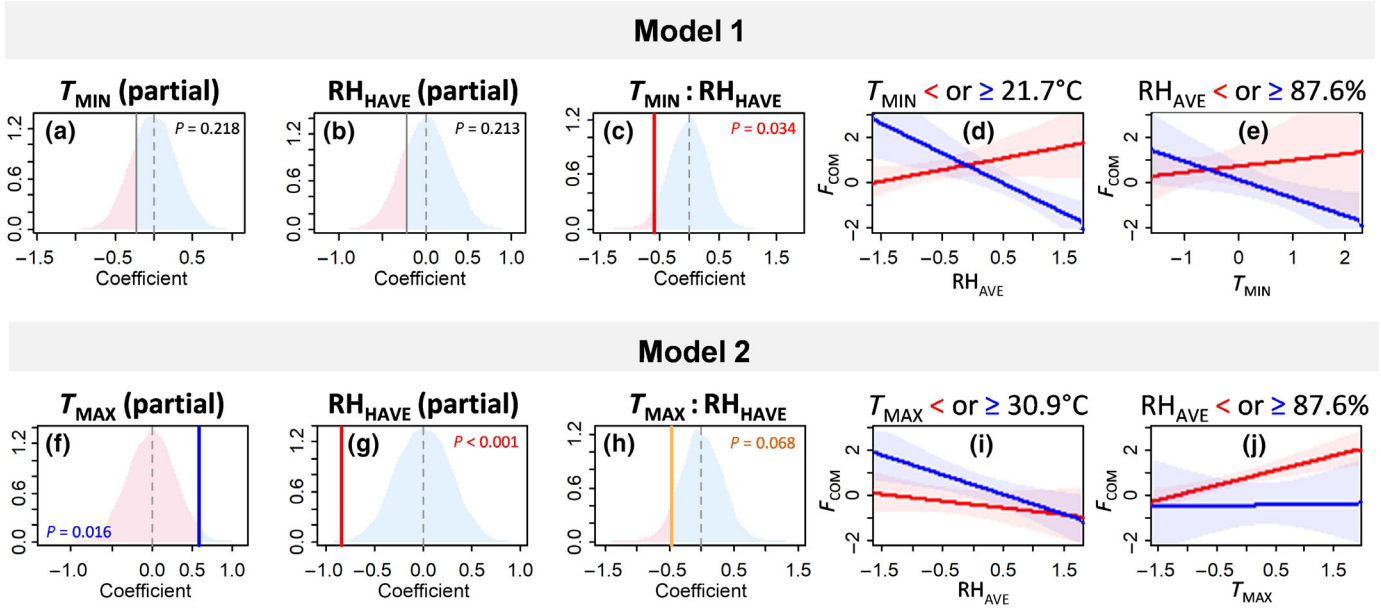

Fig. 4 Partial and interaction term slope coefficients quantifying the relative effects of two climate variables (T_{MIN} and RH_{AVE} [Model 1]; T_{MAX} and RH_{AVE} [Model 2]) on the annual community flower production (F_{COM}) (a–c; f–h). Coefficients were tested using the MSR procedure described in the Materials and Methods section (4999 randomisations). For each model, the three left graphs show the density distributions of null values for each coefficient of the model. The interaction term is written as T_{MIN} : RH_{AVE} and T_{MAX} : RH_{AVE} in Models 1 and 2, respectively. The vertical full line indicates the observed coefficient value. The line was coloured in red or blue if the coefficient value was significantly negative or positive ($P < 0.05$), respectively, and in yellow if it was negative but only marginally significant ($0.05 < P < 0.1$; see graph legend at the bottom left). The two right graphs in each model (d–e; i–j) further emphasise the OLS regression line of the F_{COM} against one climate variable of the model when the values of the other climate variable (V2) in the model were relatively low (i.e. during the 9 yr with the lowest values for V2; in red) and when the values of V2 were relatively high (i.e. the 9 yr with the highest values for V2; in blue). The shaded areas in the two right graphs represent the 95% confidence intervals in which each regression line is expected to be found.

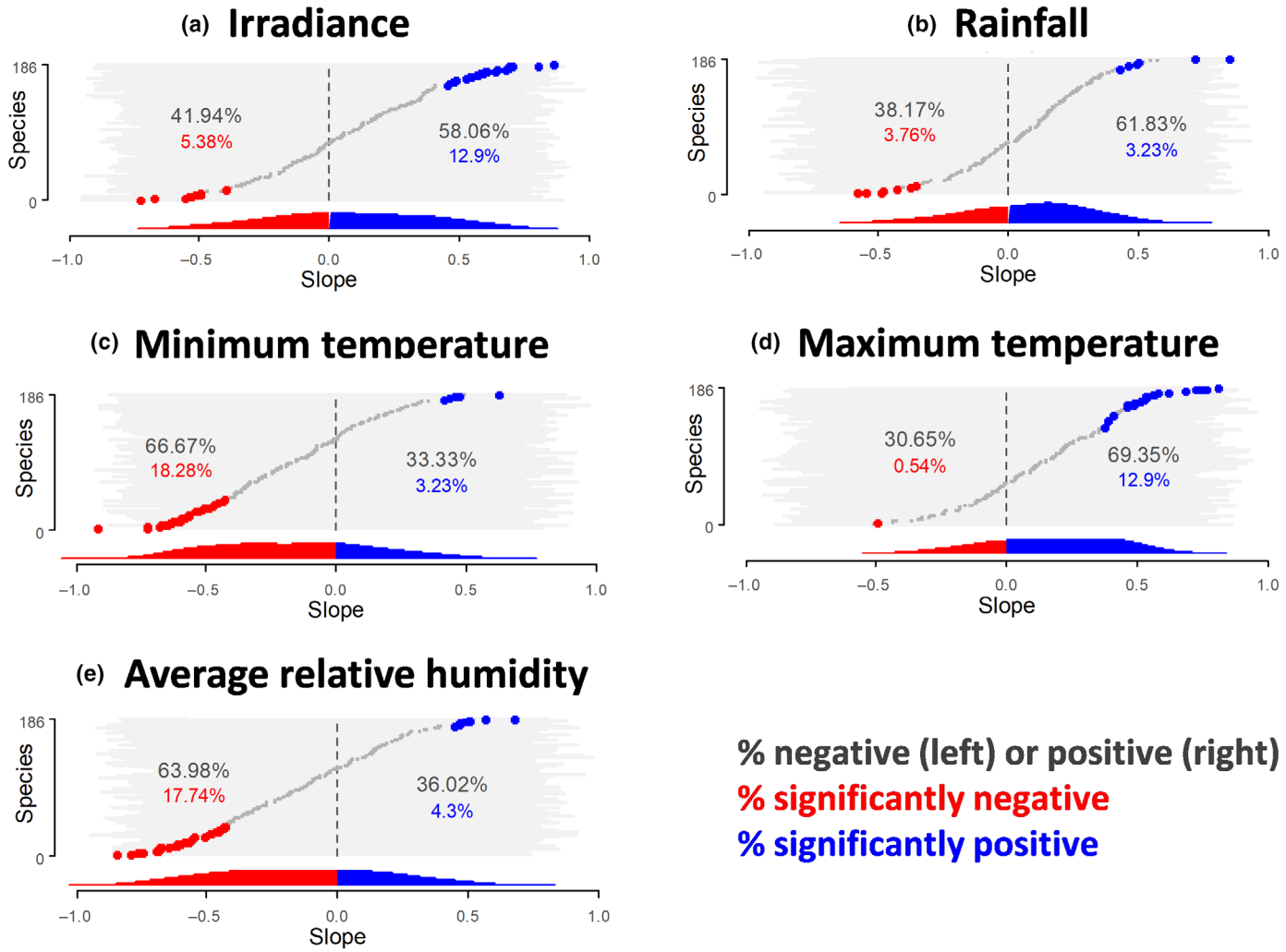

Fig. 5 Annual species flower production (F_{SPE}) response to each climate variable (a–e). Each graph shows the slope coefficients of the OLS models quantifying the effect of one climate variable on flower production, for each of the 184 species present in at least 10 phenology traps in at least 10 yr. Slope values are ordered from lowest to highest. Coloured dots indicated species with a slope value that was negative and lower than the 5–100% (red), or positive and higher than the 0–95% (blue) quantiles of 4999 null values obtained using MSR randomisations. Coloured percentages indicate the proportion of species in these groups. Grey percentages indicate the proportion of species with negative and positive slope values. The light grey shaded areas represent a piling of horizontal bars showing the whole range of null values for each species. The bottom density curve represents the density distribution of species coefficient values (equal weight among species), with the red and blue shaded areas indicating community-level differences between the proportion of negative and positive coefficients. We found no significant differences among life form guilds in species response to any climate variable, and no phylogenetic signal was observed for these responses (Supporting Information Figs S8 and S9; Notes S1).

Reduced flower production during years with warmer and wetter nights

Across species, we found that minimum temperature (T_{MIN}) and average relative humidity (RH_{AVE}) both showed negative relationships with flower production that occurred markedly more often than positive relationships (Fig. 5c,e). T_{MIN} and RH_{AVE} also showed significant negative effects at the community level (Fig. 3c,e). Increased nighttime temperatures have been shown to increase leaf dark respiration and nonphotosynthetic tissue respiration rates (Cavaleri *et al.*, 2008; Perez & Feeley, 2018). These respiratory costs reduce net primary productivity (Clark *et al.*, 2003), which is likely to affect reproductive success via decreased flower production, as suggested by our results.

In addition, we suggest the possibility that an increase in nighttime temperature has altered the responses of tree flowing to temperature as a phenological cue. Some tree species in a tropical forest in Gabon (Tutin & Fernandez, 1993) and in dipterocarp forests in Asia (Numata *et al.*, 2022) were shown to require a drop in temperature as an indication to start flowering. Shifts in the trend and variability of temperatures may disrupt such proximate cues and the timing of resource allocation to flower production.

High levels of atmospheric relative humidity reduce the gradient of vapour pressure across the leaf–atmosphere interface and hence the transpiration efficiency of plants. This may increase plant dark respiration rates (Slot *et al.*, 2014), resulting in a reduction of net photosynthesis (Cavaleri *et al.*, 2008), eventually affecting growth rate and thus potentially flower production. The

negative impact of high nighttime temperature on flower production appears to be exacerbated by high levels of humidity, as RH_{AVE} had a more pronounced negative effect on flower production when T_{MIN} was relatively high, and vice versa (Fig. 4d,e). This was expected, as leaf overheating should be exacerbated when transpiration is reduced by water-saturated conditions.

Contrary to T_{MIN}, daily maximum temperatures (T_{MAX}) at Yasuní had a positive effect more often than a negative effect among species, with roughly 24 times more species showing a significant positive response than a negative one (Fig. 5d). Yet, at the community level, no significant signal was detected (Fig. 3d). However, T_{MAX} did show a significant partial positive effect in Models 2 in Fig. 4f, implying that the T_{MAX} effect is only evident when accounting for effects of humidity. More specifically, the positive effect of T_{MAX} on flower production was more pronounced during years with the lowest average relative humidity levels (RH_{AVE}; Fig. 4j). This is partly consistent with previous evidence that suggested maximum temperature can promote flower production via both a direct increase in photosynthetic metabolism and an indirect increase in the rate of litter decomposition and nutrient recycling (Pau *et al.*, 2013). This effect is likely attenuated when evapotranspiration is reduced, that is, as air humidity gets closer to its saturation point (Damour *et al.*, 2010; Grossiord *et al.*, 2020). Our results may reveal that plants at Yasuní do not suffer as much from increases in daily temperature as they do from higher nighttime temperatures, which partly contradicts previous studies reporting that maximum temperature increase is negatively affecting primary productivity in many other tropical wet forest regions of the world (Sullivan *et al.*, 2020).

Weak impact of irradiance alone on flower production

More species responded significantly positively ($n = 24$; 12.9%) than negatively ($n = 10$; 5.4%) to solar irradiance, in terms of flower production (Fig. 5a), though we detected no significant effect of this climate variable alone at the community-level (Fig. 3a). Nevertheless, we noticed that irradiance had a significant partial positive effect in a multiple OLS model including this variable and T_{MAX} (Fig. S10), with flower production responding slightly more positively to irradiance at relatively higher T_{MAX} values. This may suggest that daytime maximum temperatures have not reached or exceeded a limit for thermal acclimation and so warmer temperatures enhance (rather than decrease) metabolic activity when irradiance levels are high. It is also worth noting that the partial positive coefficients observed for T_{MAX} (Fig. 4f) or irradiance (Fig. S10g) may potentially correlate positively with the effect of rising atmospheric CO_2 concentrations, as it has been previously reported in other tropical forests (Pau *et al.*, 2018).

Weak trend and effect of rainfall on flower production

The effect of rainfall on flower production was generally weak at both the community level (Fig. 3b) and at the species level, with few species responding significantly negatively (3.8%) or positively (3.2%; Fig. 5b). These results were consistent with our expectations, which assumed that water is not limiting at our study site.

Although we neither observed any linear trend in rainfall over the 2000–2018 period at Yasuní, nor a clear change in rainfall variability (Fig. S11), climate models predict more prolonged wet periods in the western Amazon. This would mean an increase in cloud cover, and we may expect the future climate to not only lead to a decrease in the amount of but also the seasonal variation in top-of-canopy solar irradiance. This could result in declines in the flowering production of species with high irradiance flowering optima, or species that use irradiance as a phenological cue to trigger flowering (Wright & Calderon, 2018; IPCC, 2022).

No difference in flower production responses among guilds and lineages

As noted above, species varied in the strength and direction of their flowering responses to climate variables. However, that variation could not be explained by differences in life form guild or phylogeny (Notes S1; Figs S8 and S9; Table S1). These results are consistent with previous observations that photosynthetic temperature optima are highly similar among species from various lineages and guilds with contrasting light requirement niches, including canopy and subcanopy trees and lianas (Smith *et al.*, 2017). Our results may also suggest that in Yasuní, lianas do not benefit (at least in terms of flower production) from their efficient water use that renders them highly competitive in more seasonal forests (Schnitzer & Bongers, 2011; Chen *et al.*, 2015; Smith *et al.*, 2017). We also checked whether species with different peak flowering months showed different strengths and/or signs of correlation between their annual flower production and each climate variable, but we found no significant differences (Notes S1; Fig. S8). Thus, while species do vary in their flower production responses to climate, the factors driving that variation remain unknown and further studies incorporating additional traits are needed.

Conclusion

The effects of climate change on everwet forests remain poorly studied compared with more seasonal tropical or temperate forests. Over an 18-yr period from 2000 to 2018 in a lowland everwet forest in western Amazonia, we observed a decrease in community-level flower production. This decrease in reproductive activity was accompanied by increasing temperatures and relative humidity (in addition to global increase in atmospheric CO_2 concentrations), and decreasing solar irradiance, consistent with climate predictions in this region. Flower production responses to climate variables varied across species but did not differ among different lineages and guilds. Greater nighttime temperatures and atmospheric water saturation may have negatively affected species' reproduction, via alterations of the metabolic and/or cue-based processes associated with flowering. If these trends continue, forest dynamics will likely shift, potentially altering the composition and structure of these forests in the future. Additional inventories of flowering and fruit production are needed for tropical everwet forests to better understand the

long-term impacts of climate changes on the dynamics of these valuable ecosystems.

Acknowledgements

JV was funded by a G. Evelyn Hutchinson Environmental Postdoctoral Fellowship from the Yale Institute for Biospheric Studies (Yale University, CT, USA). We thank Pablo Alvia, Alvaro Pérez, Zornitza Aguilar, Paola Barriga, Matt Priest, Caroline Whitefoord, and Gorky Villa for assistance in collecting data or identifying species; Elina Gomez for entry of trap data; Hugo Navarrete, Katya Romoleroux and the QCA herbarium staff, and David Lasso and the ECY staff for help with logistics and needed permitting; Rick Condit, Elizabeth Losos, Robin Foster, and Henrik Balslev for initial encouragement to work within the Yasuní Forest Dynamics Plot; Hugo Romero for initially summarising the YFDP and SSP weather data sets; Pablo Jarrin for setting up the TEAM weather station, and David Lasso and Carlos Padilla for maintaining that equipment and making the data available; and the Ecuadorian Ministerio del Ambiente for permission to work in Yasuní National Park. The Forest Dynamics Plot of Yasuní National Park has been made possible through the generous support of the Pontifical Catholic University of Ecuador (PUCE) funds of donaciones del impuesto a la renta, the government of Ecuador, the US National Science Foundation, the Andrew W. Mellon Foundation, the Smithsonian Tropical Research Institute, and the University of Aarhus of Denmark. The project began while NCG was at the Natural History Museum, London, with funding (2000–2004) from the Department of Botany (NHM), the Andrew W. Mellon Foundation, British Airways, and the Natural Environment Research Council (GR9/04037). It continued with NCG at Southern Illinois University Carbondale (2005–2021). We thank the Center for Tropical Forest Science for transitional funding (2006–2008, 2017–2018) and the National Science Foundation for long-term funding (2006–2020; DEB-0614525, DEB-1122634, DEB-1754632, DEB-1754668).

Competing interests

None declared.

Author contributions

JV, JAH, MRM, NCG, SAQ, LSC, RV and SJW contributed to the conception and/or design of the study. NCG, SJW, MRM, MZ, SAQ and RV are involved in field data collection. JV analysed the data with the help of JAH, LSC and SJW. JV wrote the manuscript with the help of JAH, LSC, SAQ and SJW.

ORCID

Liza S. Comita https://orcid.org/0000-0002-9169-1331
J. Aaron Hogan https://orcid.org/0000-0001-9806-3074
Margaret R. Metz https://orcid.org/0000-0002-4221-7318
Simon A. Queenborough https://orcid.org/0000-0002-2468-0958
Renato Valencia https://orcid.org/0000-0001-9770-6568
Jason Vleminckx https://orcid.org/0000-0002-7600-9170
S. Joseph Wright https://orcid.org/0000-0003-4260-5676

Data availability

The data supporting the results are archived in a Harvard Dataverse repository at doi: 10.7910/DVN/PCGFMZ.

References

Aleixo I, Norris D, Hemerik L, Barbosa A, Prata E, Costa F, Poorter L. 2019. Amazonian rainforest tree mortality driven by climate and functional traits. *Nature Climate Change* **9**: 384–388.

Allan RP. 2011. Combining satellite data and models to estimate cloud radiative effect at the surface and in the atmosphere. *Meteorological Applications* **18**: 324–333.

Baraloto C, Vleminckx J, Engel J, Petronelli P, Dávila N, Ríos M, Valderrama Sandoval EH, Mesones I, Guevara Andino JE, Fortunel C *et al.* 2021. Biogeographic history and habitat specialization shape floristic and phylogenetic composition across Amazonian forests. *Ecological Monographs* **91**: e01473.

Bauman D, Drouet T, Dray S, Vleminckx J. 2018a. Disentangling good from bad practices in the selection of spatial or phylogenetic eigenvectors. *Ecography* **41**: 1638–1649.

Bauman D, Drouet T, Fortin MJ, Dray S. 2018b. Optimizing the choice of a spatial weighting matrix in eigenvector-based methods. *Ecology* **99**: 2159–2166.

Berdugo MB, Heyer L, Contento KYS, Déleg J, Bendix J, Bader MY. 2022. High-resolution tropical rain-forest canopy climate data. *Environmental Data Science* **1**: e13.

Cavaleri MA, Oberbauer SF, Ryan MG. 2008. Foliar and ecosystem respiration in an old-growth tropical rain forest. *Plant, Cell & Environment* **31**: 473–483.

Chen Y-J, Cao K-F, Schnitzer SA, Fan Z-X, Zhang J-L, Bongers F. 2015. Water-use advantage for lianas over trees in tropical seasonal forests. *New Phytologist* **205**: 128–136.

Clark DA, Piper SC, Keeling CD, Clark DB. 2003. Tropical rain forest tree growth and atmospheric carbon dynamics linked to interannual temperature variation during 1984–2000. *Proceedings of the National Academy of Sciences, USA* **100**: 5852–5857.

Cleveland RB, Cleveland WS, McRae JE, Terpenning I. 1990. STL: a seasonal-trend decomposition. *Journal of Offical Statistics* **6**: 3–73.

Cook BI, Wolkovich EM, Davies TJ, Ault TR, Betancourt JL, Allen JM, Bolmgren K, Cleland EE, Crimmins TM, Kraft NJB *et al.* 2012. Sensitivity of spring phenology to warming across temporal and spatial climate gradients in two independent databases. *Ecosystems* **15**: 1283–1294.

Crous KY, Uddling J, De Kauwe MG. 2022. Temperature responses of photosynthesis and respiration in evergreen trees from boreal to tropical latitudes. *New Phytologist* **234**: 353–374.

Damour G, Simonneau T, Cochard H, Urban L. 2010. An overview of models of stomatal conductance at the leaf level. *Plant, Cell & Environment* **33**: 1419–1438.

Doughty CE, Goulden ML. 2008. Are tropical forests near a high temperature threshold? *Journal of Geophysical Research: Biogeosciences* **113**: G00B07.

Dray S, Legendre P, Peres-Neto PR. 2006. Spatial modelling: a comprehensive framework for principal coordinate analysis of neighbour matrices (PCNM). *Ecological Modelling* **196**: 483–493.

Duffy PB, Brando P, Asner GP, Field CB. 2015. Projections of future meteorological drought and wet periods in the Amazon. *Proceedings of the National Academy of Sciences, USA* **112**: 13172–13177.

Fassoni-Andrade AC, Fleischmann AS, Papa F, Paiva RCDD, Wongchuig S, Melack JM, Aparecida Moreira A, Paris A, Ruhoff A, Barbosa C *et al.* 2021. Amazon hydrology from space: scientific advances and future challenges. *Reviews of Geophysics* **59**: e2020RG000728.

Fleischmann AS, Papa F, Hamilton SK, Fassoni-Andrade A, Wongchuig S, Espinoza JC, Paiva RCD, Melack JM, Fluet-Chouinard E, Castello L. 2023.

Increased floodplain inundation in the Amazon since 1980. *Environmental Research Letters* **18**: 034024.

Fu R, Yin L, Li W, Arias PA, Dickinson RE, Huang L, Chakraborty S, Fernandes K, Liebmann B, Fisher R *et al.* 2013. Increased dry-season length over southern Amazonia in recent decades and its implication for future climate projection. *Proceedings of the National Academy of Sciences, USA* **110**: 18110–18115.

Funatsu BM, Le Roux R, Arvor D, Espinoza JC, Claud C, Ronchail J, Michot V, Dubreuil V. 2021. Assessing precipitation extremes (1981–2018) and deep convective activity (2002–2018) in the Amazon region with CHIRPS and AMSU data. *Climate Dynamics* **57**: 827–849.

Garwood NC, Metz MR, Queenborough SA, Persson V, Wright SJ, Burslem DF, Zambrano M, Valencia R. 2023. Seasonality of reproduction in an ever-wet lowland tropical forest in Amazonian Ecuador. *Ecology* **104**: e4133.

Grossiord C, Buckley TN, Cernusak LA, Novick KA, Poulter B, Siegwolf RTW, Sperry JS, McDowell NG. 2020. Plant responses to rising vapor pressure deficit. *New Phytologist* **226**: 1550–1566.

Haghtalab N, Moore N, Heerspink BP, Hyndman DW. 2020. Evaluating spatial patterns in precipitation trends across the Amazon basin driven by land cover and global scale forcings. *Theoretical and Applied Climatology* **140**: 411–427.

Hoorn C, Wesselingh FP, ter Steege H, Bermudez MA, Mora A, Sevink J, Sanmartín I, Sanchez-Meseguer A, Anderson CL, Figueiredo JP *et al.* 2010. Amazonia through time: Andean uplift, climate change, landscape evolution, and biodiversity. *Science* **330**: 927–931.

IPCC. 2022. Impacts, Adaptation, and Vulnerability. In: Pörtner HO, Roberts DC, Tignor M, Poloczanska ES, Mintenbeck K, Alegría A, Craig M, Langsdorf S, Löschke S, Möller V, eds. *Contribution of Working Group II to the Sixth Assessment Report of the Intergovernmental Panel on Climate Change*. Cambridge, UK; New York, NY, USA: Cambridge University Press, 3056 pp.

Jimenez JC, Libonati R, Peres LF. 2018. Droughts over Amazonia in 2005, 2010, and 2015: a cloud cover perspective. *Frontiers in Earth Science* **6**: 227.

Krause GH, Winter K, Krause B, Jahns P, García M, Aranda J, Virgo A. 2010. High-temperature tolerance of a tropical tree, *Ficus insipida*: methodological reassessment and climate change considerations. *Functional Plant Biology* **37**: 890–900.

Lin H, Chen Y, Zhang H, Fu P, Fan Z. 2017. Stronger cooling effects of transpiration and leaf physical traits of plants from a hot dry habitat than from a hot wet habitat. *Functional Ecology* **31**: 2202–2211.

Loescher HW, Oberbauer SF, Gholz HL, Clark DB. 2003. Environmental controls on wet ecosystem-level carbon exchange and productivity in a Central American tropical wet forest. *Global Change Biology* **9**: 396–412.

Malo G, Arguello C. 1984. *Proyecto Oriente, Mapa de Compilación Geológica de la Provincia Del Napo*. Quito, Ecador: Departamento de Geología, Instituto Ecuatoriano de Minería, Ministerio de Energía y Minas.

Marengo JA, Souza CM Jr, Thonicke K, Burton C, Halladay K, Betts RA, Alves LM, Soares WR. 2018. Changes in climate and land use over the Amazon region: current and future variability and trends. *Frontiers in Earth Science* **6**: 228.

McGregor GR, Niewold S. 1998. *Tropical climatology: an introduction to the climates of the low latitudes, 2nd edn*. Chichester, UK: John Wiley & Sons, 352 pp.

Min Q, Joseph E, Duan M. 2004. Retrievals of thin cloud optical depth from a multifilter rotating shadowband radiometer. *Journal of Geophysical Research: Atmospheres* **109**: 3964.

Needham J, Merow C, Chang-Yang CH, Caswell H, McMahon SM. 2018. Inferring forest fate from demographic data: from vital rates to population dynamic models. *Proceedings of the Royal Society B: Biological Sciences* **285**: 20172050.

Netherly PJ. 1997. Loma y ribera: patrones de asentamiento prehistóricos en la Amazonia Ecuatoriana. *Fronteras de Investigación* **1**: 33–54.

Numata S, Yamaguchi K, Shimizu M, Sakurai G, Morimoto A, Alias N, Zaimah Noor Azman N, Hosaka T, Satake A. 2022. Impacts of climate change on reproductive phenology in tropical rainforests of Southeast Asia. *Communications Biology* **5**: 311.

Pan Y, Birdsey RA, Fang J, Houghton R, Kauppi PE, Kurz WA, Phillips OL, Shvidenko A, Lewis SL, Canadell JG *et al.* 2011. A large and persistent carbon sink in the world's forests. *Science* **333**: 988–993.

Parry IM, Ritchie PDL, Cox PM. 2022. Evidence of localised Amazon rainforest dieback in CMIP6 models. *Earth System Dynamics* **13**: 1667–1675.

Parsons LA. 2020. Implications of CMIP6 projected drying trends for 21st century Amazonian drought risk. *Earth's Future* **8**: e2020EF001608.

Pau S, Okamoto DK, Calderón O, Wright SJ. 2018. Long-term increases in tropical flowering activity across growth forms in response to rising CO_2 and climate change. *Global Change Biology* **24**: 2105–2116.

Pau S, Wolkovich EM, Cook BI, Nytch CJ, Regetz J, Zimmerman JK, Wright SJ. 2013. Clouds and temperature drive dynamic changes in tropical flower production. *Nature Climate Change* **3**: 838–842.

Perez TM, Feeley KJ. 2018. Increasing humidity threatens tropical rainforests. *Frontiers in Ecology and Evolution* **6**: 68.

Pitman NCA. 2000. *A large-scale Inventory of two Amazonian tree communities*. PhD thesis, Duke University, Duke, NC, USA.

Queenborough SA, Burslem DFRP, Garwood NC, Valencia R. 2007. Habitat niche partitioning by 16 species of Myristicaceae in Amazonian Ecuador. *Plant Ecology* **192**: 193–207.

Rodwell L, Lee KJ, Romaniuk H, Carlin JB. 2014. Comparison of methods for imputing limited-range variables: a simulation study. *BMC Medical Research Methodology* **14**: 1–11.

Satake A, Chen YY, Fletcher C, Kosugi Y. 2019. Drought and cool temperature cue general flowering synergistically in the aseasonal tropical forests of Southeast Asia. *Ecological Research* **34**: 40–49.

Schnitzer SA, Bongers F. 2011. Increasing liana abundance and biomass in tropical forests: emerging patterns and putative mechanisms. *Ecology Letters* **14**: 397–406.

Schrodt F, Kattge J, Shan H, Fazayeli F, Joswig J, Banerjee A, Reichstein M, Bönisch G, Díaz S, Dickie J *et al.* 2015. BHPMF–a hierarchical B ayesian approach to gap-filling and trait prediction for macroecology and functional biogeography. *Global Ecology and Biogeography* **24**: 1510–1521.

Slot M, Rey-Sánchez C, Gerber S, Lichstein JW, Winter K, Kitajima K. 2014. Thermal acclimation of leaf respiration of tropical trees and lianas: response to experimental canopy warming, and consequences for tropical forest carbon balance. *Global Change Biology* **20**: 2915–2926.

Smith JR, Queenborough SA, Alvia P, Romero-Saltos H, Valencia R. 2017. Testing the Liana Dominance hypothesis: no strong evidence for increasing liana abundance in the Myristicaceae of a neotropical Aseasonal rain forest. *Ecology* **98**: 456–466.

Smith MN, Taylor TC, van Haren J, Rosolem R, Restrepo-Coupe N, Adams J, Wu J, de Oliveira RC, da Silva R, de Araujo AC *et al.* 2020. Empirical evidence for resilience of tropical forest photosynthesis in a warmer world. *Nature Plants* **6**: 1225–1230.

Sterck F, Anten NP, Schieving F, Zuidema PA. 2016. Trait acclimation mitigates mortality risks of tropical canopy trees under global warming. *Frontiers in Plant Science* **7**: 607.

Sullivan MJ, Lewis SL, Affum-Baffoe K, Castilho C, Costa F, Sanchez AC, Ewango CEN, Hubau W, Marimon B, Monteagudo-Mendoza A *et al.* 2020. Long-term thermal sensitivity of Earth's tropical forests. *Science* **368**: 869–874.

Tibbitts TW. 1979. Humidity and plants. *Bioscience* **29**: 358–363.

Tutin CEG, Fernandez M. 1993. Relationships between minimum temperature and fruit production in some tropical forest trees in Gabon. *Journal of Tropical Ecology* **9**: 241–248.

Valencia R, Condit RS, Romoleroux K, Villa Muñoz G, Svenning J-C, Magard E, Bass MS, Losos E, Balslev H. 2004a. Yasuní forest dynamics plot, Ecuador. In: Losos EC, Leigh EG, eds. *Tropical forest diversity and dynamism: findings from a large-scale plot network*. Chicago, IL, USA: University of Chicago Press, 609–620.

Valencia R, Foster RB, Villa G, Condit R, Svenning JC, Hernández C, Romoleroux K, Losos E, Magard E, Balslev H. 2004b. Tree species distributions and local habitat variation in the Amazon: large forest plot in eastern Ecuador. *Journal of Ecology* **92**: 214–229.

Van Schaik CP, Terborgh JW, Wright SJ. 1993. The Phenology of Tropical Forests: adaptive significance and consequences for primary consumers. *Annual Review of Ecology and Systematics* **24**: 353–377.

Vinod N, Slot M, McGregor IR, Ordway EM, Smith MN, Taylor TC, Sack L, Buckley TN, Anderson-Teixeira KJ. 2022. Thermal sensitivity across forest

vertical profiles: patterns, mechanisms, and ecological implications. *New Phytologist* **237**: 22–47.

Wagner HH, Dray S. 2015. Generating spatially constrained null models for irregularly spaced data using Moran spectral randomization methods. *Methods in Ecology and Evolution* **6**: 1169–1178.

Walter H, Harnickell E, Mueller-Dombois D. 1975. *Climate-diagram maps of the ecological regions of the earth*. Berlin, Germany: Springer.

Williamson GB, Laurance WF, Oliveira AA, Delamônica P, Gascon C, Lovejoy TE, Pohl L. 2000. Amazonian tree mortality during the 1997 El Nino drought. *Conservation Biology* **14**: 1538–1542.

Wright SJ, Calderon O. 1995. Phylogenetic patterns among tropical flowering phenologies. *Journal of Ecology* **83**: 937–948.

Wright SJ, Calderon O. 2006. Seasonal, El Niño and longer term changes in flower and seed production in a moist tropical forest. *Ecology Letters* **9**: 35–44.

Wright SJ, Calderon O. 2018. Solar irradiance as the proximate cue for flowering in a tropical moist forest. *Biotropica* **50**: 374–383.

Supporting Information

Additional Supporting Information may be found online in the Supporting Information section at the end of the article.

Dataset S1 List of species with their family and additional sampling information.

Dataset S2 Phenological data.

Dataset S3 Climate data.

Dataset S4 Flowering species composition data for each census.

Dataset S5 List of species names with corresponding acronyms.

Fig. S1 Patterns of missing values among climate variables before imputation.

Fig. S2 Observed and imputed mean monthly values of each climate variable across the study period.

Fig. S3 *Post hoc* analyses evaluating the reliability of the imputations of the missing climate variable values.

Fig. S4 Total number of flowering trap–census observations for each species for each year.

Fig. S5 Mean number of trap–census flowering observations for each month and each species.

Fig. S6 Visual comparison of the temporal variation of irradiance before and after MSR randomisation.

Fig. S7 Slope coefficient quantifying the effect of each climate variable on flower production, with or without a 1-yr time lag between the response and the explanatory variable.

Fig. S8 Comparison of annual species flower production response to each climate variable among guilds and seasonal flowering optima.

Fig. S9 Phylogeny and species response to each climate variable.

Fig. S10 Slope coefficients examining the relative effects of two climate variables (T_{MIN} and irradiance, and T_{MAX} and irradiance) on the annual community flower production.

Fig. S11 Mean annual rainfall amounts for each year of the study period.

Methods S1 R code used to perform our data analysis.

Notes S1 Comparison of flower production response to climate variables across guilds, lineages, and according to the peak flowering month of species.

Table S1 Tests of the phylogenetic signal for the effect of each climate variable on flower production.

Please note: Wiley is not responsible for the content or functionality of any Supporting Information supplied by the authors. Any queries (other than missing material) should be directed to the *New Phytologist* Central Office.